Nanoscale

ARTICLE

Self-assembling Venturi-like peptide nanotubes

Alberto Fuertes, Haxel Lionel Ozores, Manuel Amorín,* Juan R. Granja*

Received 00th January 20xx,
Accepted 00th January 20xx

DOI: 10.1039/x0xx00000x

www.rsc.org/

We describe the design and synthesis of self-assembling peptide nanotubes with an internal filter area and whose length and internal diameters, at the entrance and in the constricted area, are precisely controlled

Introduction

Nanotubes are hollow cylindrical materials of nanoscopic dimensions. The materials from which the nanotubes are made define the properties of the internal and external surfaces. In addition, nanotube properties also depend on the length and internal diameter. Among the well-known carbon nanotubes,[1] peptide nanotubes represent one of the most nanotechnologically relevant materials because of their unique properties.[2] These materials are generally prepared using small peptides that, under appropriate conditions, self-assemble to form the tubular structure. Therefore, the nanotubes can be designed in such a way that its assembly and disassembly is controlled by external signals. Nanotubes made by the stacking of cyclic peptide nanotubes (self-assembling cyclic peptide nanotubes, SCPNs) represent a unique approach because of the precise control of the nanotube internal diameter, which depends exclusively on the peptide ring size.[3] SCPNs are made from cyclic components that adopt a flat conformation in which all of the residue side chains are oriented radially and point outward. The perpendicular orientation of amide bonds (carbonyl and NH) allows the formation of face-to-face hydrogen bonds with two neighboring CPs.

One of the limitations of the nanotubes made by stacking rings is the lack of control over their length. Once the nanotube is formed there is no precise way to control the number of stacked subunits. Recently, it has been shown that the use of cyclic peptide-polymer hybrids with different polymer sizes allowed some control of the length, although this aspect has not been completely resolved yet.[4] In this regard, different transport rates were observed in transmembrane nanotubes depending on the number of CP subunits that form the nanotube.[5] These membrane nanotubes mimic the structure and properties of natural ion channels.[6] Although the SCPNs compete with them in the transport efficiency of alkali ions, the ion selectivity is far from the natural systems. In addition, studies carried out with transmembrane SCPNs have shown that some transport selectivity can be achieved playing with nanotube internal diameter,[5] e.g., decapeptides efficiently transported glucose or glutamic acid while octapeptides did not.[7]

The remarkable combination of efficiency and transport selectivity of natural ions channel continues spurring the scientific interest in the design of improved artificial systems.[6] Some of the protein channels, such as potassium channels,[8] have a shape characterized by the presence of a selectivity filter in the centre of the channel that is preceded by a dilated water-filled chamber. Therefore the form of the internal cavity of these proteins resembles the shape of Venturi tubes. These tubes are straight hollow structures with a constricted middle section. This shape accelerates the fluid stream creating a region of low pressure. They are mainly used in processes that do not tolerate a permanent pressure loss or require the maximum accuracy for highly viscous liquids. The use of this shape in natural channels might be related with the ability to reduce the fluid pressure to ensure the ion selectivity. Therefore the construction of simple tube model with this shape might provide a new tool to study the transport mechanism of membrane proteins. Here we present a new way to control the nanotube dimensions by using as basic components covalently linked CP dimers. Each cyclic component has different diameter and self-assembling properties. This design also provides the opportunity to generate nanotubes with cavities composed by a central narrow area, the selective filter, and open and wide entries. This Venturi-like peptide nanotubes might have applications in the design of improved transmembrane channel transporters or new porous membranes.[7,9]

Singular Research Centre in Chemical Biology and Molecular Materials, (CIQUS), Organic Chemistry Department, University of Santiago de Compostela (USC), 15782 Santiago de Compostela, Spain.

† Footnotes relating to the title and/or authors should appear here.
Electronic Supplementary Information (ESI) available: [details of any supplementary information available should be included here]. See DOI: 10.1039/x0xx00000x

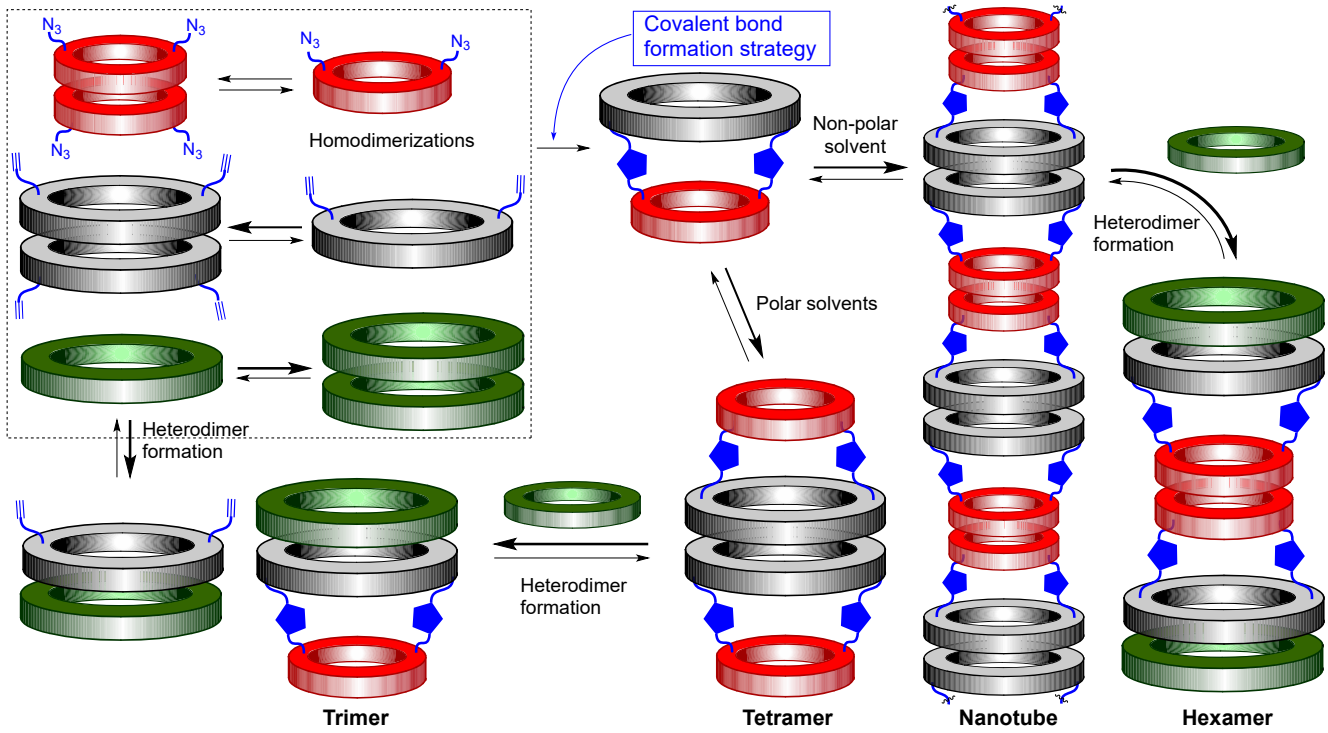

Scheme 1. General strategy for the preparation of Venturi-like self-assembling cyclic peptide nanotubes (SCPNs) with precise length control and constricted sections (selective filter). Green colour was used to denote the complementary Ach-based octapeptide (**CP3**), the grey for the Acp-based octapeptide (**CP2**) with large dimerization constant and the red colour was used to denote the small CP (**CP1**).

Results and discussion

Design concepts

In an effort to overcome the problem of controlling nanotube length, we designed a novel dimeric component that combines two covalently linked cyclic peptides with different structural and supramolecular properties (Scheme 1). The two CPs that consist of cyclic γ-amino acids (γ-Aca) alternated with α-amino acids (α,γ-CPs)[10] were designed to dimerize through an antiparallel β-type interaction. The larger of the two CPs was selected to have a large homodimerization constant.[11] In addition, this peptide has the ability to form heterodimeric aggregates that are even more stable than the corresponding homodimer.[11b] The second CP was chosen due to its small internal diameter and dimerization constant.[12] The weakness of these association properties would allow regulation of its self-assembly properties through modification of the conditions or polarity of the media. In previous years, we have shown that this type of peptides can form nanotubes, most probably due to their propensity to adopt the flat conformation.[13] The CPs were linked through the substituents located on the amide backbone, which are oriented perpendicular to the ring plane. These substituents bear chemoselective and complementary reactive groups, such as an azide and an acetylene moiety for use in copper(I)-catalyzed azide–alkyne cycloaddition (CuAAC).[14] These design principles led us to select a cyclic tetrapeptide (**CP1**, Scheme 2) for regulation of the self-assembly process and also to create the narrow orifice of the selective filter in the nanotube channel.[12] The larger component was chosen to be an octapeptide (**CP2**) bearing two propargyl moieties placed at the first and third γ-Aca while the other two would be N-methylated. The tetrapeptide would contain two 3-azidopropyl groups located on the amide skeleton. In order to facilitate homo- and hetero-dimerization selectivity, it was decided to prepare the octapeptide using 3-aminocyclopentane-carboxylic acid (γ-Acp) that, in addition to the formation of the corresponding homodimer, interacts with octapeptides constituted by 3-aminocyclohexanecarboxylic acids (γ-Ach) to form heterodimeric aggregates that are more stable than the corresponding homodimer.[11] For this purpose a third peptide (**CP3**), made of γ-Ach residues, was also used.

Synthetic studies and dimer characterization

Cyclic peptides **CP1**, **CP2** and **CP3**[11a] (Scheme 2) were prepared by the synthetic sequence illustrated in Schemes 1SI, 2SI and

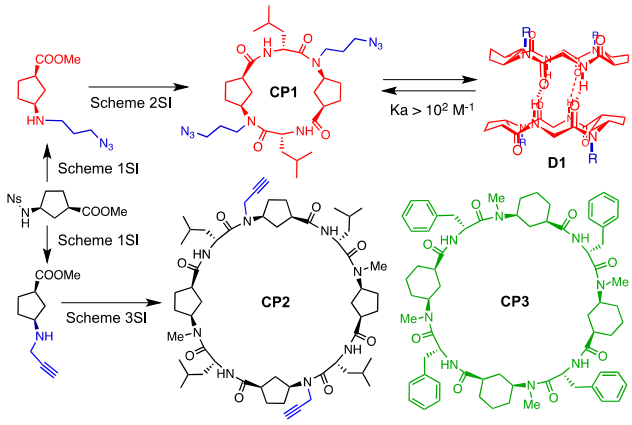

Scheme 2. Structures of cyclic peptides (CP1, CP2 and CP3) used in this work. CP1 and CP2 were prepared using the Nosyl derivative of Acp.

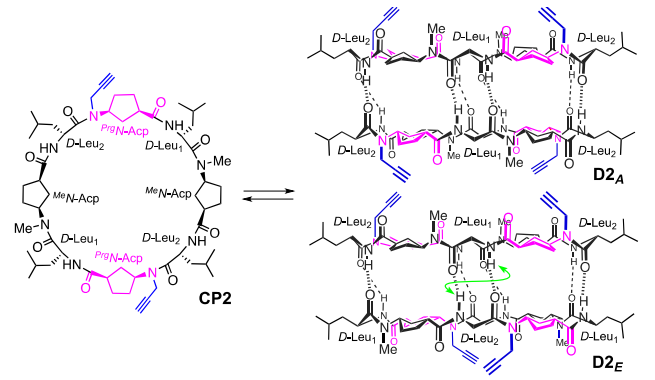

Scheme 3. Structure of the two non-equivalent dimers of CP2. The eclipsed dimer ($D2_E$), in which the two N-propargylated Acp residues (in magenta) lie on top of each other, and the alternated dimer ($D2_A$), in which the N-methylated and N-propargylated Acp residues are paired. The green arrow denotes the nOe cross peak observed in the ROESY experiment (Fig 1a). Magenta colour was used to remark the relative orientation of N-propargylated Acp residues.

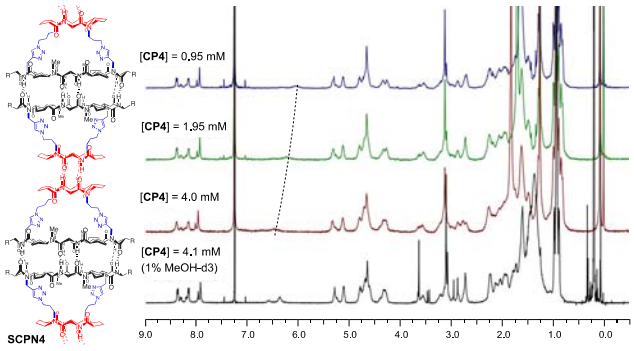

Fig. 2. Structure of self-assembling cyclic peptide nanotube **SCPN4** and ^{1}H NMR spectra of **CP4** at different concentrations (1–4 mM, from top to bottom) and in the presence of 1% methanol d_3 (bottom) – conditions in which only **D4** exists. The dashed line on the spectra remark the down-field shift of the amide proton corresponding to the small CP of **CP4** upon increasing its concentration.

3SI in the supporting information. The key reaction was the Fukuyama sulfonamide alkylation[15] (see Scheme 1SI) for the preparation of γ-amino acids bearing the propargyl and 3-azidopropyl groups.[16]

As expected, **CP1** forms in deuterochloroform the corresponding dimer (**D1**, Scheme 2), as confirmed by proton NMR experiments. The downfield shift of the amide proton signals on increasing the concentration of **CP1**, from 6.30 ppm at a concentration of 1.1 mM to 7.32 ppm at 41.1 mM, reflects the dimerization through intermolecular hydrogen bonds at room temperature (Fig. 1SI in supporting information). This concentration-dependent chemical shift allowed a dimerization constant K_a of 330 M^{-1} to be determined in chloroform at 298 K. A series of experiments carried out at different temperatures in the range 233–313 K allowed the corresponding thermodynamic parameters ΔH°_{298} = –22.1 kJ mol^{-1} and ΔS°_{298} = –26.0 J K^{-1} mol^{-1} to be extracted from van't Hoff plots (Fig. 2SI). The dimerization process, as expected, is enthalpy driven with an estimated energy per hydrogen bond of 5.52 kJ mol^{-1}, which is higher than those for other peptides of this type.[11] Furthermore, the β-sheet-like nature was supported by FT-IR, with bands for amide I and amide II_{II} at 1624 and 1528 cm^{-1}, respectively, together with an amide A band around 3301 cm^{-1}.[17]

The octapeptide **CP2** also dimerizes but in this case the assembly process generates two non-superimposable dimers ($D2_A$ and $D2_E$) due to the C2 symmetry of **CP2** (Scheme 3). The two forms can be distinguished because of their slow interconversion on the NMR time scale and are denoted by the splitting of the signals of the amide protons with signals at 8.35 and 8.14 ppm for the major dimer ($D2_E$) and 8.26 and 8.20 ppm for the minor one ($D2_A$). The major isomer was assigned as the eclipsed form ($D2_E$) due to the nOe cross peak observed between the two non-equivalent leucines (Figure 1). The proton NMR spectra are independent of the cyclic peptide concentration even after the addition of up to 20% methanol, thus confirming that the association constant in chloroform must be larger than 10^5 M^{-1}. In fact, previous studies on cyclic octapeptides provided values of the association constant larger than 10^8 M^{-1}.[11b]

Once the self-assembling properties of the basic components of our design had been confirmed, the next step was to link these units covalently. Unfortunately, the low solubility of the CPs precluded the use of typical aqueous click conditions.[14]

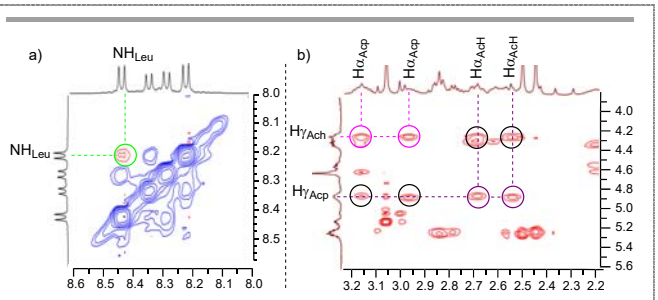

Fig. 1. a) ROESY and b) NOESY spectra of homodimer **D2** and heterodimer **D3-4**, respectively, in which cross peaks between the NH of the non-equivalent Leu (green) and the cross strand $H\gamma_{Ach}$-$H\alpha_{Acp}$ (magenta) $H\gamma_{Acp}$-$H\alpha_{Ach}$ (purple) are shown. The black circles indicate the $H\gamma_{Acp}$-$H\alpha_{Acp}$ and $H\gamma_{Ach}$-$H\alpha_{Ach}$ cross peaks characteristic of each CP.

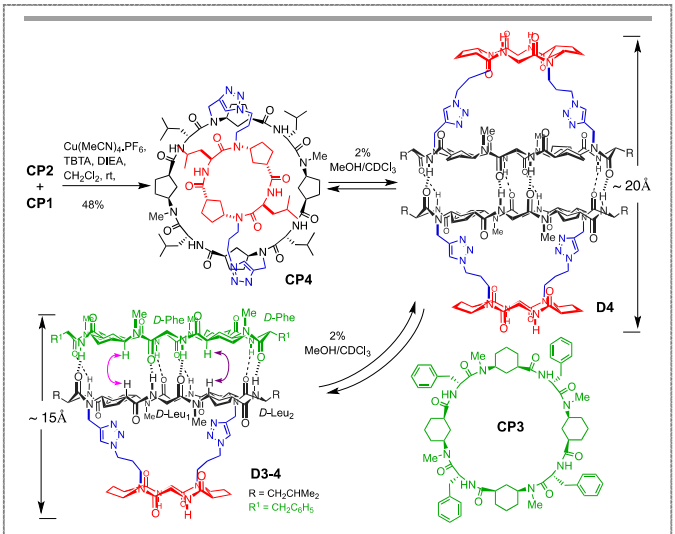

Scheme 4. Structure of covalently linked CPs (**CP4**), model of one of the corresponding dimers ($D4_A$) formed in chloroform solution containing methanol and the heterodimeric structure formed by CPs **CP3** and **CP4** (**D3-4**). Coloured arrows indicate the observed nOe cross peaks in the NOESY experiment (Fig. 1b).

Finally, the reaction of **CP1** and **CP2** in the presence of tetrakis(acetonitrile)-copper(I) hexafluorophosphate, tris[(1-benzyl-1*H*-1,2,3-triazol-4-yl)methyl] amine (TBTA) and diisopropylethylamine in dichloromethane provided **CP4** in 48% yield (Scheme 4).[18] This compound has low solubility in non-polar organic solvents (< 4.0 mM in $CDCl_3$) and the ^1H NMR spectrum contains broad signals, which suggest the formation of long aggregates (**SCPN4**, Fig. 2). At low concentration (1 mM) two sets of signals corresponding to the two non-equivalent interactions between the octapeptide rings, the alternated and eclipsed forms, can be differentiated. Two broad signals corresponding to the tetrapeptide amide protons can also be identified. The chemical shifts of these signals, as for **CP1**, are dependent on the concentration of **CP4** and the temperature, with a change from 5.78 ppm at 40 °C for 1 mM to 6.48 ppm at 4 mM and 20 °C (Figure 2). This fact confirms the assembling properties through the small CP. The splitting of the amide proton signal of the small CP into two separate signals is caused by the existence of two different β-sheet interactions through the octapeptide. The addition of a small amount of methanol led to a ^1H NMR spectrum with sharp peaks, the chemical shifts of which were independent of the peptide concentration (Figure 2). This finding shows that, under these conditions, the tetrapeptide is no longer involved in the self-assembly process and nanotube formation. On the other hand, the two sets of signals derived from octamer dimerization are still present, thus confirming the formation of the tetrameric aggregates $\mathbf{D4_A}$ and $\mathbf{D4_E}$ (Scheme 4). The resulting nanotube has the narrow component located at the entrance of the channel and it has an estimated length of 20 Å. The addition of **CP3** to a $CDCl_3$ solution of **CP4** containing 5% methanol gave a new supramolecular entity. The ^1H NMR spectrum contained a new set of signals while those corresponding to the tetrameric nanotube disappeared (Scheme 5 and Fig. 3SI). The four doublets (8.61, 8.58, 8.44 and 8.42 ppm) correspond to the amide protons of the two non-equivalent Leucines and the de-symmetrized Phe. The nOe cross peaks between the Hγ protons of one cyclic peptide and Hα of the other cyclic peptide (Fig. 1b) can only be explained by the formation of the heterodimeric nanotube made of three stacks with an estimated length of around 15 Å.

The nanotube formed by six stacked cyclic peptides [**D(D3-4)**, Scheme 5] with an estimated length of 30 Å was also prepared. In this particular case, a suspension of **SCPN4** in deuterochloroform was treated with increasing amounts of **CP3**. The ^1H NMR spectra showed the appearance of new doublets at 8.66, 8.60, 8.48 and 8.39 ppm, which correspond to the NHs of both octapeptides. The chemical shifts are similar to those of the previously mentioned **D(D3-4)** in 1% MeOH/$CDCl_3$. The main difference with respect to the trimeric nanotube is the chemical shift of amide protons of the tetrapeptide. In pure $CDCl_3$ the NH chemical shift is concentration-dependent – as one would expect given its participation in the self-assembly process. The estimated association constant in $CDCl_3$ from the concentration-dependence experiments is 340 M^{-1}, very similar to the tetrapeptide by itself (**CP1**), confirming that the attachment of the octapeptide **CP3** did not interfere in the structure and

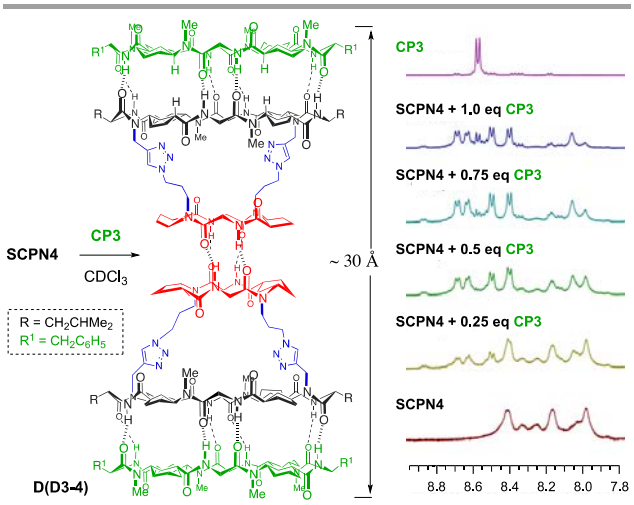

Scheme 5. Left, structure of the 30 Å long SCPN made by dimerization of **D3-4** in a non-polar solvent ($CDCl_3$). On the right, the ^1H NMR region between 8.95 and 7.80 ppm is shown, where the NH signals of **SCPN4** disappear, upon addition of different amounts of **CP3** (spectrum shown at the top). Full spectra can be found at Fig 3SI.

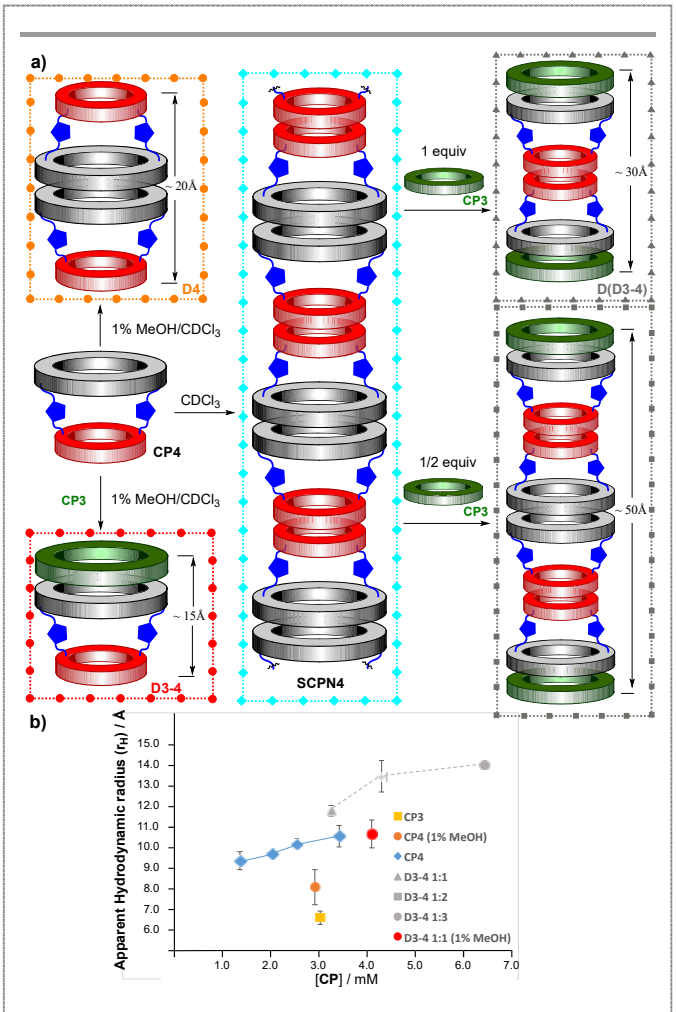

Scheme 6. a) Model of the proposed tubular structures formed by the assembly process of **CP3** and **CP4**. b) Plot of the different r_H values obtained from DOSY NMR measurements for several species in solution (pure $CDCl_3$ unless otherwise specified) at different concentrations.

assembly properties of the tetrapeptide component.

With this qualitative information in hand, we explored an alternative method to quantify the size (length) of the supramolecular aggregates. To this end, Diffusion Ordered Spectroscopy (DOSY) was carried out on samples containing different concentrations of **CP4** in $CDCl_3$ (Scheme 6). The observed small association constant through the tetrapeptide determined that the number of stacked peptide subunits depends on the concentration of dimer **CP4**. The nanotube length must increase on increasing the concentration of **CP4** and therefore diffusion experiments could provide information about the length of **SCPN4**. Due to the fast equilibrium exchange between monomers and supramolecular nanotubes through the tetramer association, the samples are constituted by the distribution of all supramolecular species (monomer, dimers, trimers and so on). Therefore the observed diffusion coefficient values obtained are the numerical average of all the diffusion rates of each component of the mixture. The self-diffusion rates obtained in DOSY experiments were compared with those measured for an internal standard [tetrakis(trimethylsilyl)silane, TMSS] and the results were used to estimate the apparent hydrodynamic radii (r_H) of the species formed in solution using equation (1), which is derived from an approximation to the Einstein–Stokes equation (see SI).[19]

$$D_{TMSS} / D_x = (c_{CP} \cdot f_{s,CP} \cdot r_{H,CP}) / (c_{TMS} \cdot f_{s,TMSS} \cdot r_{H,TMSS}) \qquad (1)$$

Where r_H is the hydrodynamic radius, c is a numerical factor that depends on the ratio between the size of the species and the size of the solvent molecules and f_s accounts for the asymmetry in the shape of the tubular aggregates.[20]

Due to the structural characteristics of nanotubes with variable lengths but a fixed diameter, the changes in hydrodynamic ratios are derived from the increase in number of CP subunits alone. The low solubility of **CP4** in non-polar solvents (< 4 mM) limited the ensemble sizes to those whose length and diameter are similar. As a consequence, f_s values of 1.00 were used for experiments carried out with only **CP4**. For the larger nanotubes, i.e., those derived from the 1:3 ratio between **CP3** and **CP4**, we used a value of 1.05 to account for the ellipsoidal molecular form of the objects.[21] The length must be restricted to multiples of the inter-ring distance of each peptide (4.85 Å) stacked in the SCPN.[5,13,22] Therefore the nanotubes made of two, three, four or six cyclic peptides would correspond lengths of approximately 10, 15, 20 or 30 Å, respectively.

Table 1 Results of the DOSY experiments

Sample	[a]	[CP] mM	Additive	Diffusion ratio Dst/Dmu	*fs*	r_h Å
CP4	◆	3.5	-	2.99	1	10.61
CP4	◆	2.6	-	2.88	1	10.24
CP4	◆	2.1	-	2.74	1	9.74
CP4	◆	1.4	-	2.65	1	9.42
CP4	●	3.0	MeOH[c]	2.29	1	8.13
CP3/CP4 (1:1)	▲	4.2	-	3.34	1	11.88
CP3/CP4 (1:2)	■	4.4	-	4.00	1.05	13.54
CP3/CP4 (1:3)	●	6.6	-	4.17	1.05	14.12
CP3/CP4 (1:1)	●	4.2	MeOH[c]	3.02	1	10.74
CP3	■	3.1	-	1.87	1	6.65

[a] symbols used in graphic of Scheme 6, [b] We selected the following signals trying to maximize the S/N ratio (non-overlapped simple and intense signals): singlet at 0.22 ppm for TMS and N-Me of CPs (3.13 ppm for **CP3** and 3.06 ppm for the mixture of **CP3** and **CP4**), [c] DOSY experiments were carried out in the presence of 1% MeOH.

The apparent r_H in the presence of a 1% MeOH d_3 solution in chloroform, conditions in which **CP4** forms **D4** exclusively, was measured to be 8.13 ± 0.91 Å. This is compatible with the estimated size of dimer **D4** (Scheme 6b). In deuterochloroform, the r_H of **CP4** increased with increasing concentration, thus confirming the formation of the longer supramolecular structure at higher concentrations. The radius r_H ranged from 10.61 ± 0.52 Å at 3.5 mM to 9.42 ± 0.44 Å at 1.4 mM. In any case, all of the measurements in this range revealed larger radii in pure $CDCl_3$ than their counterpart with 1% MeOH. In parallel, the addition of 0.33, 0.66 and 1 equivalents of **CP3** to a solution of **CP4** in $CDCl_3$ gave rise to r_H values of 14.12 ± 0.07, 13.54 ± 0.80 and 11.88 ± 0.26 Å, clearly indicating that the stoichiometry between the two species has a direct influence on the length of the aggregate. On employing sub-stoichiometric amounts of **CP3**, the free **D4** subunit can be inserted into **D(D3-4)** to form longer nanotubes and the ratio between the free **D4** subunit and dimer **D(D3-4)** is mainly responsible for the resulting nanotube length (Scheme 6).

Conclusions

We have prepared a new class of self-assembling peptide nanotubes based on covalently linked cyclic peptides. The dimeric peptide is constituted by two peptides with orthogonal self-assembling properties that allow the precise control of the nanotube structural properties. Therefore, the strategy allows the generation of selective filter areas in the nanotube internal cavity, Venturi-like peptide nanotubes, by selecting peptides of different sizes. The orthogonal assembly properties also allow control of the nanotube length. The combination of a covalent dimer with a second peptide with complementary assembly properties to one of the components provided additional control. In this way, nanotubes with lengths ranging from 15 to 50 Å were prepared. This strategy may have applications for the design of improved transmembrane channel transporters or new porous membranes with improved properties. Our efforts in these directions will be reported in due course.

Acknowledgements

This work was supported by the Spanish Ministry of Economy and Competitivity (Mineco) and the ERDF (CTQ2013-43264-R), and by the Xunta de Galicia and the ERDF (EM2014/011). A. F.

and H. L. O. thank Mineco for their FPU contracts. We also thank the ORFEO-CINCA network and Mineco (CTQ2014-51912-REDC). We very much appreciate Dr. Ignacio Alfonso (IQAC-CSIC) for his help in designing DOSY experiments.

Notes and references

1 M. S. Saito, R. Dresselhaus, G. M. Dresselhaus, *Physical Properties of Carbon Nanotubes*; Imperial College Press: London, 1998.

2 a) I. W. Hamley, *Angew. Chem. Int. Ed.* 2014, **53**, 6866–6881; b) T. Shimizu, H. Minamikawa, M. Kogiso, M. Aoyagi, N. Kameta, W. Ding, M. Masuda, *Pol. J.* 2014, **46**, 831–858; c) R. García-Fandiño, M. Amorín, J. R. Granja, "Synthesis of Supramolecular Nanotubes" in *Supramolecular Chemistry: From Molecules to Nanomaterials.* P. A. Gale, J. W. Steed, Eds. John Wiley & Sons Ltd, Chichester, UK, 2012, *Vol 5*, pp 2149–2182.

3 a) R. J. Brea, C. Reiriz, J. R. Granja, *Chem. Soc. Rev.* 2010, **39**, 1448–1456; b) R. Chapman, M. Danial, M. L. Koh, K. A. Jolliffe, S. Perrier, *Chem. Soc. Rev.* 2012, **41**, 6023–6041.

4 a) R. Chapman, M. L. Koh, G. G. Warr, K. A. Jolliffe, S. Perrier, *Chem. Sci.* 2013, **4**, 2581–2589; b) J. Couet, M. Biesalski, *Small* 2008, **4**, 1008–1016; c) R. Chapman, K. A. Jolliffe, S. Perrier, *Polym. Chem.* 2011, **2**, 1956–1963.

5 a) J. Montenegro, M. R. Ghadiri, J. R. Granja, *Acc. Chem. Res.* 2013, **46**, 2955–2965; b) M. R. Ghadiri, J. R. Granja and L. K. Buehler, *Nature* 1994, **369**, 301–304.

6 N. Rodríguez-Vázquez, A. Fuertes, M. Amorín, J. R. Granja, "Bioinspired Artificial Sodium and Potassium Ion Channels" in The Alkali Metal Ions: Their Role for Life. A. Sigel, H. Sigel, R. K. O. Sigel, Eds. Springer Int., Cham, Switzerland, 2016, *Vol 16*, pp 485-556.

7 a) J. R. Granja, M. R. Ghadiri, *J. Am. Chem. Soc.* 1994, **116**, 10785–10786; b) J. Sanchez-Quesada, H. S. Kim, M. R. Ghadiri, *Angew. Chem. Int. Ed.* 2001, **40**, 2503–2506.

8 D. A. Doyle, J. O. M. Cabral, R. A. Pfuetzner, A. Kuo, J. M. Gulbis, S. L. Cohen, B. T. Chait, R. MacKinnon, *Science* 2008, **280**, 69–77.

9 M. Amorín, A. Pérez, J. Barberá, H. L. Ozores, J. L. Serrano, J. R. Granja and T. Sierra, *Chem. Commun.* 2014, **50**, 688-690.

10 a) M. Amorín, L. Castedo, J. R. Granja, *J. Am. Chem. Soc*. 2003, **125**, 2844–2845; b) R. J. Brea, M. Amorín, L. Castedo, J. R. Granja, *Angew. Chem. Int. Ed.* 2005, **44**, 5710–5713.

11 a) M. Amorín, L. Castedo, J. R. Granja, *Chem.–Eur. J.* 2005, **11**, 6543–6551; b) R. J. Brea, M. J. Pérez-Alvite, M. Panciera, M. Mosquera, L. Castedo, J. R. Granja, *Chem.–Asian J.* 2011, **6**, 110–121; c) R. García Fandiño, L. Castedo, J. R.Granja, S. A. Vázquez, *J. Phys. Chem. B* 2010, **114**, 4973–4983.

12 a) M. Amorín, R. J. Brea, L. Castedo, J. R. Granja, *Org. Lett.* 2005, **7**, 4681–4684; b) C. Reiriz, M. Amorín, R. García-Fandiño, L. Castedo, J. R. Granja, *Org. Biomol. Chem.* 2009, **7**, 4358–4361; c) M. Amorín, R. J. Brea, L. Castedo, J. R. Granja, *Heterocyclic* 2006, **67**, 575–583.

13 a) C. Reiriz, R. J. Brea, R. Arranz, J. L. Carrascosa, A. Garibotti, B. Manning, J. M. Valpuesta, R. Eritja, L. Castedo, J. R. Granja, *J. Am. Chem. Soc.* 2009, **131**, 11335–11337; b) R. Garcia-Fandino, M. Amorín, L. Castedo, J. R. Granja, *Chem. Sci.* 2012, **3**, 3280–3285; c) J. Montenegro, C. Vázquez-Vázquez, A. Kalinin, K. E. Geckeler, J. R. Granja, *J. Am. Chem. Soc.* 2014, **136**, 2484–2491; d) M. Cuerva, R. García Fandiño, C. Vázquez-Vázquez, M. A. López-Quintela, J. Montenegro, J. R. Granja, *ACS Nano* 2015, **9**, 10834–10843.

14 a) H. C. Kolb, M. G. Finn, K. B. Sharpless, *Angew. Chem. Int. Ed.* 2001, **40**, 2004–2021; b) V. V. Rostovtsev, L. G. Green, V. V. Fokin, K. B. Sharpless, *Angew. Chem. Int. Ed.* 2002, **41**, 2596–2599; c) C. W. Tornøe, C. Christensen, M. Meldal, *J. Org. Chem*. 2002, **67**, 3057–3064.

15 a) T. Fukuyama, C. K. Jow, M. Cheung, *Tetrahedron Lett.* 1995, **36**, 6373–6374; b) T. Fukuyama, M. Cheung, C. K. Jow, Y. Hidai, T. Kan, *Tetrahedron Lett.* 1997, **38**, 5831–5834.

16 a) N. Rodríguez-Vázquez, S. Salzinger, L. F. Silva, M. Amorín, J. R. Granja, *Eur. J. Org. Chem.* 2013, 3477–3482; b) N. Rodríguez-Vázquez, R. García-Fandiño, M. Amorín, J. R. Granja, *Chem. Sci.* 2016, **7**, 183–187.

17 a) P. I. Haris, D. Chapman, *Biopolymers (Peptide Sci.)* 1995, **37**, 251–263; b) S. Krimm, J. Bandekar in *Advances in Protein Chemistry* (Eds.: C. B. Anfinsen, J. T. Edsall, F. M. Richards), Academic Press, Orlando, FL, 1986, pp 181 –364; c) A. Barth, C. Zscherp, *Quart. Rev. Biophys.* 2002, **35**, 369–430.

18 S. C. Picot, B. R. Mullaney, P. D. Beer, *Chem.–Eur. J.* 2012, **18**, 6230–6237.

19 a) A. Macchioni, G. Ciancaleoni, C. Zuccaccia, D. Zuccaccia, *Chem. Soc. Rev.* 2008, **37**, 479–489; b) D. Zuccaccia, A. Macchioni, *Organometallics* 2005, **24**, 3476–3486.

20 M. M. Tirado, C. López Martínez, J. J. García de la Torre, *Chem. Phys.* 1984, **81**, 2074–2052.

21 a) L. Allouche, A. Marquis, J.-M. Lehn, *Chem.–Eur. J.* 2006, **12**, 7520–7525; b) A. Wong, R. Ida, L. Spindler, G. Wu, *J. Am. Chem. Soc.* 2005, **127**, 6990–6998.

22 T. D. Clark, J.M. Buriak, K. Kobayashi, M. P. Isler, D. E. McRee, M. R. Ghadiri, *J. Am. Chem. Soc.* 1998, **120**, 8949–8962.

